INFECTION AND IMMUNITY, July 2009, p. 2624–2634 Vol. 77, No. 7
0019-9567/09/$08.00+0 doi:10.1128/IAI.01531-08
Copyright © 2009, American Society for Microbiology. All Rights Reserved.

Subcellular Localization of the *Staphylococcus aureus* Heme Iron Transport Components IsdA and IsdB[▽]†

Gleb Pishchany, Susan E. Dickey, and Eric P. Skaar*

Department of Microbiology and Immunology, Vanderbilt University Medical School, Nashville, Tennessee 37232-2605

Received 17 December 2008/Returned for modification 28 January 2009/Accepted 16 April 2009

Staphylococcus aureus **is a human pathogen that represents a tremendous threat to global public health. An important aspect of *S. aureus* pathogenicity is the ability to acquire iron from its host during infection. In vertebrates, iron is sequestered predominantly within heme, the majority of which is bound by hemoglobin. To acquire iron, *S. aureus* binds hemoglobin, removes heme, and transports it into the cytoplasm, where heme is degraded. This process is carried out by the iron-regulated surface determinant system (Isd); however, the mechanism by which hemoglobin recognition occurs is not completely understood. Here we report that the surface receptor components of the Isd system, IsdA and IsdB, physically interact with each other and are anchored to a discrete location within the cell wall. This organized localization pattern is dependent upon the iron status of the bacterium. Furthermore, we have found that hemoglobin colocalizes with IsdB at discrete sites within the cell wall. Virulence studies revealed that IsdB is required for the efficient colonization of the heart and that IsdB is differentially expressed within infected organs, suggesting that *S. aureus* experiences various degrees of iron starvation depending on the site of infection. These findings significantly expand our understanding of hemoglobin iron acquisition and demonstrate an orchestrated pattern of regulation and localization for the *S. aureus* heme iron acquisition system.**

Staphylococcus aureus is a commensal organism that colonizes the anterior nares of approximately 30% of the human population (26). *S. aureus* is also an important human pathogen that is capable of infecting virtually any site of the body (23–25). The shift from commensal colonizer to invading pathogen typically occurs upon a breakage of the skin or mucosal barrier, whereupon *S. aureus* employs an arsenal of virulence factors that allow it to survive within the host and cause considerable damage (29). The majority of these virulence factors are either secreted from the bacterial cell or anchored to the cell wall through the action of transpeptidases known as sortases (29, 30). The functions of cell wall-anchored proteins include adherence, immune evasion, nutrient acquisition, and resistance to antimicrobials, all processes important for the survival of *S. aureus* in the context of infection (6, 7, 14, 16, 19, 31–33, 35, 39, 40, 46). The contribution of cell wall-anchored proteins to the pathogenicity of *S. aureus* is evident through a decrease in the virulence of sortase mutants in animal models of infection (21, 22, 30, 32, 49). Among the functions carried out by sortase-anchored proteins is the acquisition of iron (31), which is a vital nutrient that is concealed from invading bacteria by host iron-sequestering proteins in a process known as nutritional immunity (2, 9).

Most iron within the mammalian host is contained within the tetrapyrrole heme, the cofactor of hemoglobin (8, 11, 47). Hemoglobin is a sufficient source of iron in vitro for many bacterial pathogens including *S. aureus* (9, 46). *S. aureus* acquires iron from hemoglobin through the cooperative action of the iron-regulated surface determinant (Isd) system, which is conserved in many gram-positive pathogens (31, 44). The critical first step in this process of heme iron acquisition is hemoglobin binding to its receptors IsdB and IsdH (HarA) (12, 31, 36, 46). IsdB and IsdH then remove heme and pass it to the surface-exposed protein IsdA or to IsdC, which is embedded within the cell wall (34, 36, 50). IsdC in turn passes heme to the IsdDEF membrane transporter, which pumps heme into the cytoplasm, where it is degraded by the heme oxygenases IsdG and IsdI (34, 37, 43, 50). IsdB is required for hemoglobin binding and utilization as an iron source, while IsdA, IsdE, IsdG, and IsdI are necessary for heme iron utilization (19, 20, 28, 37, 46). The proposed model for heme iron transport through the Isd system predicts that the protein constituents of the Isd system physically interact with each other to form a molecular conduit for heme transport through the cell wall. However, the subcellular localization pattern of the Isd proteins has not been reported. In addition, it is not known if proteins of the Isd system physically engage with one another within the bacterium. Finally, the contribution of hemoglobin capture to staphylococcal virulence is incompletely defined.

Here we demonstrate that IsdA and IsdB colocalize to discrete sites within the staphylococcal cell wall, and these sites correspond to regions of hemoglobin capture. IsdAB localization and subsequent hemoglobin binding are regulated by iron availability and appear to occur at the site of new cell wall formation. In support of this localization pattern, we demonstrate that IsdA and IsdB physically interact within the staphylococcal cell wall, providing direct evidence that proteins of the Isd system act as a coordinated unit to mediate hemoglobin recognition and heme iron acquisition. Finally, we report that IsdB exhibits an organ-specific regulation pattern, which cor-

* Corresponding author. Mailing address: Department of Microbiology and Immunology, Vanderbilt University Medical School, 21st Avenue South, Medical Center North, Room A-5102A, Nashville, TN 37232. Phone: (615) 343-0002. Fax: (615) 343-7392. E-mail: Eric.Skaar@vanderbilt.edu.

† Supplemental material for this article may be found at http://iai.asm.org/.

▽ Published ahead of print on 27 April 2009.

responds to an organ-specific requirement for IsdB during the pathogenesis of *S. aureus*. Taken together, these results expand our understanding of the mechanism and function of hemoglobin capture by gram-positive pathogens.

MATERIALS AND METHODS

Bacterial strains and growth conditions. All experiments were carried out with *S. aureus* strain Newman or with mutants generated in its background. The protein A knockout mutant (Δ*spa* mutant) was generated through allelic replacement as previously described (1). Briefly, *spa* and approximately 1 kb of flanking DNA were cloned into pCR2.1. The primers used were spa-51-AttB1 (GGGG ACAAGTTTGTACAAAAAAGCAGGCTTCGAAGTAAAATTGATGA GCG) and spa-32-AttB2 (GGGGACCACTTTGTACAAGAAAGCTGGGTCA ACCTGGAGGTGCACTTG). The plasmid was then digested with NruI and Bpu10I, which excised *spa*; treated with T4 DNA polymerase to generate blunt ends; and religated. The resulting construct was recombined into pKOR1 and used for allelic replacement in Newman (1). Strains inactivated for *spa isdB*, *spa isdA*, and *spa isdAB* were generated by transducing the Δ*isdB*::*ermC*, Δ*isdA*::*ermC*, or Δ*isdAB*::*ermC* allele into the Δ*spa* background using bacteriophage ϕ-85 (31) to create Δ*spa* Δ*isdB*, Δ*spa* Δ*isdA*, and Δ*spa* Δ*isdAB*. A strain inactivated for *spa isdB isdH* was generated by transducing Δ*spa* Δ*isdB* with the Δ*isdH*::*tetR* allele (kindly provided by Eszter Nagy) to create Δ*spa* Δ*isdB* Δ*isdH* using similar techniques (12). All transductions were confirmed by PCR and/or immunoblotting. All *S. aureus* cultures were inoculated from a single colony and grown overnight (~15 h) in 5 ml tryptic soy broth (TSB) in 15-ml conical tubes at 37°C with shaking at 180 rpm unless noted otherwise.

Immunofluorescence. Bacteria were grown overnight in 5 ml TSB or TSB supplemented with 2,2-dipyridyl (DIP) in 15-ml conical tubes at 37°C with shaking at 180 rpm. Bacteria were sedimented at 3,000 × *g* for 5 min and washed three times in 1 volume of ice-cold phosphate-buffered saline (PBS) (pH 7.4). The following procedures were carried out at room temperature. One hundred fifty microliters of bacteria was applied onto poly-L-lysine-coated coverslips for 5 min. The coverslips were then floated on 2% formaldehyde in PBS for 20 min to fix the bacteria. Coverslips were then washed once with PBS and blocked in PBS plus 3% (wt/vol) bovine serum albumin (BSA) for 1 h. Coverslips were then incubated with BSA and primary antibody, washed three times with PBS, incubated in BSA with secondary antibody, washed three times, sealed onto a slide by nail polish, and visualized using an Olympus BX60 microscope. Pictures were taken with an Olympus DP71 camera using DP Controller and analyzed using DP Manager software. For the simultaneous labeling of IsdB and hemoglobin, the primary antibodies were added simultaneously, followed by the secondary antibodies. For the simultaneous labeling of IsdA and IsdB, IsdA antibody was biotinylated by use of an EZ-Link NHS-PEO solid-phase biotinylation kit. The labeling included four successive incubations: (i) rabbit anti-IsdB, (ii) anti-rabbit-488, (iii) rabbit biotinylated anti-IsdA, and (iv) streptavidin-Alexa Fluor 555. The antibodies and concentrations used for immunofluorescence were as follows: 1:5,000 for rabbit anti-IsdB, 1:15,000 for rabbit anti-IsdA (31), 1:250 for mouse anti-human hemoglobin (Santa Cruz), 1:50 for rabbit biotinylated anti-IsdA, 1:250 for Alexa Fluor 488 goat anti-rabbit immunoglobulin G (IgG) (H+L) (green), 1:250 for Alexa Fluor 488 goat anti-mouse IgG(H+L), 1:250 for Alexa Fluor 555 goat anti-rabbit IgG(H+L) (red), and 1:250 for streptavidin-Alexa Fluor 555.

FACS assay. For fluorescence-activated cell sorter (FACS) assays, the cells were labeled similarly to the method described above for immunofluorescence except that bacteria were fixed and incubated with antibodies in solution as opposed to on coverslips. The antibodies and concentrations used were similar to those used for immunofluorescence with the exception of hemoglobin labeling, where all antibodies were used at a 1:1,000 dilution. The cells were fixed with 2% formaldehyde for the second time after labeling. FACS analysis was performed with a FACSCalibur system (BD) using Cell Quest Pro software. The mean fluorescence intensity was quantified with Flow Explorer 4.2.

Hemoglobin binding. For hemoglobin binding assays, cultures grown overnight were spun down for 5 min at 3,000 × *g* and resuspended in 1 volume of PBS (pH 7.4) containing 0.5 μM hemoglobin (Sigma) for immunofluorescence and 1 μM hemoglobin for FACS analysis. The cultures were then incubated at room temperature for 0.5 h on a rotisserie, washed in PBS, and labeled for hemoglobin as described above for immunofluorescence.

Fluorescent hemoglobin binding assay. Human hemoglobin was conjugated to a fluorescent molecule with a DyLight 549 Microscale antibody labeling kit (Pierce) in borate buffer (pH 8.5) according to the manufacturer's recommendations. Forty microliters of the cultures grown overnight in TSB plus 1 mM DIP was resuspended in 40 μl borate buffer containing 4 μM labeled hemoglobin and incubated at room temperature for 30 min. The samples were then washed three times in borate buffer and fixed with 2% formaldehyde in PBS in a 100-μl volume. The cells were attached to coverslips and visualized. In competition assays, unlabeled hemoglobin was added at 12 μM, while BSA was added at 50 μM.

Trypsin treatment. *S. aureus* cultures grown overnight were resuspended in 1 volume of PBS plus 250 μg/ml trypsin (Sigma). The suspension was incubated at 37°C with shaking for 1 h. Cells were then washed three times with PBS containing 1 mM phenylmethylsulfonyl fluoride (PMSF) followed by incubation at 37°C with shaking in TSB with 1 mM DIP and 1 mM PMSF. Aliquots were taken after 0, 5, 15, 30, and 60 min of incubation; immediately placed on ice; and washed with ice-cold PBS three times. Once all the samples were collected, they were processed for immunofluorescence.

Immunogold labeling and electron microscopy. For immunogold labeling, the primary-antibody concentrations and incubation times were the same as those described above for immunofluorescence. Bacterial cells were attached to poly-L-lysine-coated nickel Formvar grids. The samples were fixed with 2% formaldehyde in sodium cacodylate buffer. The secondary antibody, 6-nm colloidal gold-Affinipure goat anti-rabbit IgG (H+L), was used at a 1:50 dilution. Blocking and antibody labeling were carried out in TBS (pH 7.1) plus 3% BSA. After all labeling and washing steps, the grids were briefly washed three times with double-deionized water. Samples were viewed using an FEI (Hillsboro, OR) CM12 transmission electron microscope.

Immunoblotting. Immunoblotting was performed using nitrocellulose membranes. Membranes were blocked with 5% milk made in TBS with 0.1% Tween 20 (TBST) from 1 h to overnight. The membranes were then incubated in milk plus primary antibody, washed three times with TBST, incubated in milk plus secondary antibody, and washed three times in TBST. Membranes were visualized using an Odyssey infrared imaging system (Li-Cor), which was also used to quantify intensities of the blots. The antibodies used for immunoblotting were rabbit anti-IsdB (1:10,000), rabbit anti-IsdA (1:25,000), and Alexa Fluor 680 goat anti-rabbit IgG(H+L) (1:25,000).

Immunoprecipitation. Immunoprecipitation was carried out using a protein A Seize X kit (Pierce). Agarose beads were cross-linked to anti-IsdB according to the manufacturer's recommendations. Briefly, 35 μl of anti-IsdB antiserum was bound to 200 μl of the beads and cross-linked by 25 μl disuccinimidyl suberate. *S. aureus* cultures grown overnight were resuspended in 1 ml TSM (100 mM Tris [pH 7.0], 500 mM sucrose, 10 mM $MgCl_2$) containing 20 μg lysostaphin and incubated at 37°C for 1 h. PMSF was added to 100 μM upon the completion of incubation. The protoplasts were pelleted at 16,000 × *g* for 2 min. Two hundred microliters of the supernatant was mixed with 200 μl PBS (400 μl total) and loaded onto a column containing 50 μl agarose-protein A beads cross-linked to anti-IsdB. The samples were incubated at 4°C overnight on a rotisserie. The beads were then washed five times with PBS, and bound proteins were eluted three times under conditions of low pH in 150-μl volumes for each elution. The elution samples were pooled together (elution 1). The beads were then transferred into a microcentrifuge tube and boiled for 5 min in 100 μl of a solution containing 4% (wt/vol) sodium dodecyl sulfate (SDS) and 0.5 M Tris (pH 8.0). This fraction was added to the pooled fractions eluted under conditions of low pH (elution 2). The samples were normalized before loading onto 12% SDS-polyacrylamide gel electrophoresis (PAGE) gels. The immunoprecipitation of recombinant IsdA (rIsdA) (15 μM) with rIsdB (7.5 μM) (31) was carried out in a similar manner, with the omission of elution 2. The proteins were mixed and incubated at 37°C for 0.5 h prior to immunoprecipitation.

Systemic mouse infections. Six- to eight-week old C57BL/6J mice were infected retro-orbitally with ~10^7 CFU grown to mid-log phase and resuspended in sterile PBS. Ninety-six hours postinfection, the mice were euthanized with forced inhalation of CO_2. The hearts and livers were removed postmortem and homogenized in 1 ml PBS for further processing. For immunofluorescence and quantification of IsdA and IsdB, the homogenized organs of four infected mice were transferred into microcentrifuge tubes and centrifuged at 1,000 × *g* for 1 min. The supernatant was transferred into another tube and centrifuged for 3 min at 16,000 × *g*. The supernatant was decanted, and the pellet was resuspended in 1 ml PBS and spun again at 16,000 × *g* for 3 min. The supernatant was removed, and the pellet was resuspended in 200 μl TSM. Twenty microliters was removed to determine the CFU/ml of the samples. Twenty micrograms of lysostaphin was added to the remaining suspension (final concentration, 100 μg/ml lysostaphin) and incubated at 37°C for 1 h. PMSF was added to 1 mM, and the samples were frozen at −20°C. The following morning, the CFU/ml were quantified, and normalized samples were assessed for relative amounts of IsdB and IsdA in the infected organs by quantitative immunoblotting. For immunofluorescence, the samples were not treated with lysostaphin but rather were prepared

for visualization using a fluorescent microscope. CFU/ml were quantified by serial dilutions in PBS and plating onto tryptic soy agar. Each group included at least nine mice.

RESULTS

IsdB surface expression is regulated by iron availability. Proteins of the Isd system are likely to be targeted to the same subcellular locale in order to ensure the efficient acquisition of heme iron. To test the hypothesis that the cell wall-anchored Isd proteins are proximal to each other, we chose to use immunofluorescence. Proteins of the Isd system are upregulated under low-iron conditions; therefore, we grew *S. aureus* cultures in TSB supplemented with the iron chelator DIP. IsdB expression on the staphylococcal surface was evaluated using IsdB-specific rabbit antiserum (anti-IsdB) and a secondary antibody conjugated to a fluorophore. As expected for these conditions, the primary antibody bound to the surface of *S. aureus* (Fig. 1A). To control for nonspecific binding of anti-IsdB, we tested antibody binding to Δ*isdB* cells grown in TSB plus DIP and wild-type *S. aureus* cells grown in iron-sufficient TSB, a growth condition that is not permissive to IsdB expression (31, 46). Anti-IsdB bound to *S. aureus* cells under all of these conditions, indicating significant nonspecific binding in these experiments (Fig. 1A to C).

S. aureus protein A is a cell wall factor that nonspecifically binds the constant regions of IgG (16). We reasoned that protein A might be responsible for the nonspecific labeling observed upon staining with anti-IsdB (15). To circumvent this issue, we created an *S. aureus* strain that was inactivated for the gene encoding protein A (Δ*spa*) and analyzed IsdB expression. Immunoblotting demonstrated that the inactivation of *spa* does not affect the expression of IsdB (data not shown). Δ*spa* cells expressed IsdB on the surface when grown under iron-depleted conditions, whereas IsdB was not detectable when Δ*spa* cells were grown under iron-sufficient conditions (Fig. 1D and E). In addition, the Δ*spa* Δ*isdB* strain did not elaborate an IsdB signal regardless of the iron status of the bacterium (Fig. 1F). To quantify the effects of the *spa* deletion on IsdB detection, we performed a FACS assay on *S. aureus* cells grown under both iron-sufficient and iron-depleted conditions (Fig. 1G). These experiments confirmed that IsdB is expressed on the surface of *S. aureus* cells in an iron-dependent manner, and alterations in iron status lead to an approximately 19-fold change in IsdB surface expression as measured by FACS. Taken together, these results establish that iron restriction increases the expression and surface anchoring of IsdB.

Subcellular distribution of IsdA and IsdB is regulated by iron availability. In order to determine how iron availability affects the localization of the Isd system on the surface of *S. aureus*, we grew Δ*spa* cultures overnight in TSB supplemented with various concentrations of DIP. As expected, we were unable to detect IsdB on the surface of *S. aureus* cells grown under iron-sufficient conditions (Fig. 2A). Bacteria grown in increasing concentrations of iron chelator exhibited a commensurate increase in levels of IsdB expression and surface anchoring (Fig. 2C). Furthermore, the addition of excess iron to medium containing DIP suppressed IsdB expression, eliminating the possibility that IsdB upregulation was induced by DIP independently of its iron-chelating activity (Fig. 2A and C). During the course of these experiments, it was noted that the distribution pattern of IsdB on the surface of staphylococci is affected by the iron status of the organism. More specifically, at 250 μM DIP, IsdB localizes to discrete puncta throughout the cell surface, whereas *S. aureus* cells grown with 1 mM DIP distribute IsdB in a uniform circumferential pattern around the cell wall (Fig. 2A). A similar pattern of IsdB expression and surface localization was observed upon iron starvation induced by a different iron chelator [ethylenediamine-di(*o*-hydroxyphenylacetic acid)] (data not shown).

To determine if this iron-dependent localization pattern was specific to IsdB, we analyzed IsdA expression and distribution

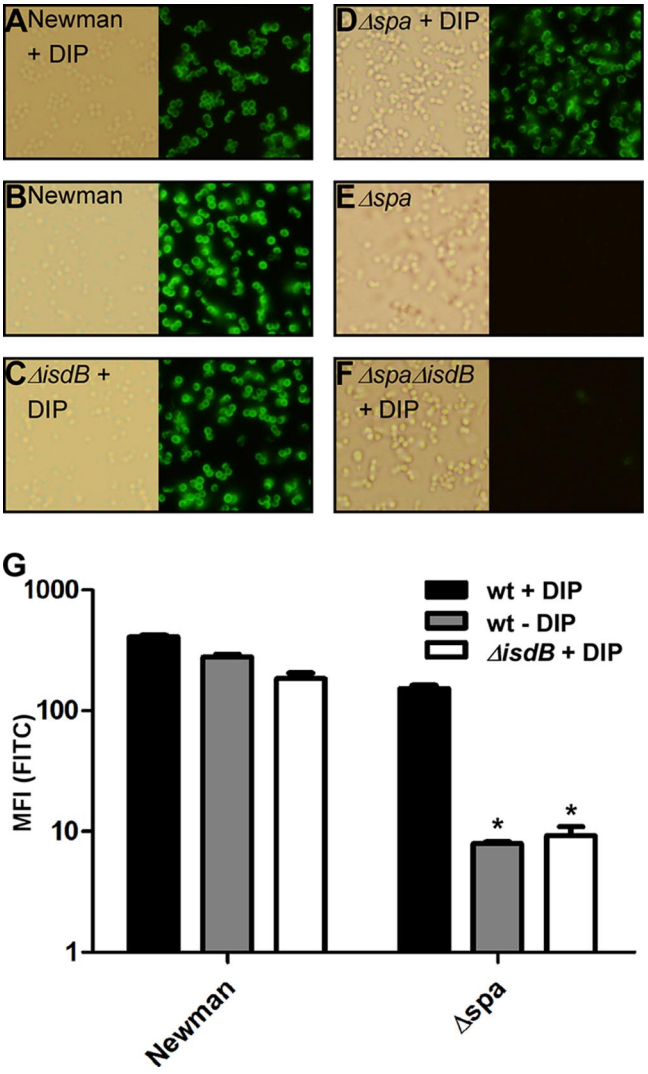

FIG. 1. Creation of a protein A-deficient strain for specific labeling of *S. aureus* surface-exposed proteins. (A to F) *S. aureus* strains were grown overnight in TSB with 1 mM of the iron-chelating agent DIP where indicated. Bacteria were subsequently labeled with rabbit anti-IsdB antibody and Alexa Fluor 488 goat anti-rabbit IgG(H+L). (G) Bacteria grown under the same conditions and labeled similarly to A to F were subjected to FACS analysis to determine mean fluorescence intensity (MFI). Error bars represent standard errors. Asterisks indicate statistically significant differences in relation to Δ*spa* cells with DIP as determined by a Student's *t* test ($P < 0.05$). FITC, fluorescein isothiocyanate; wt, wild type.

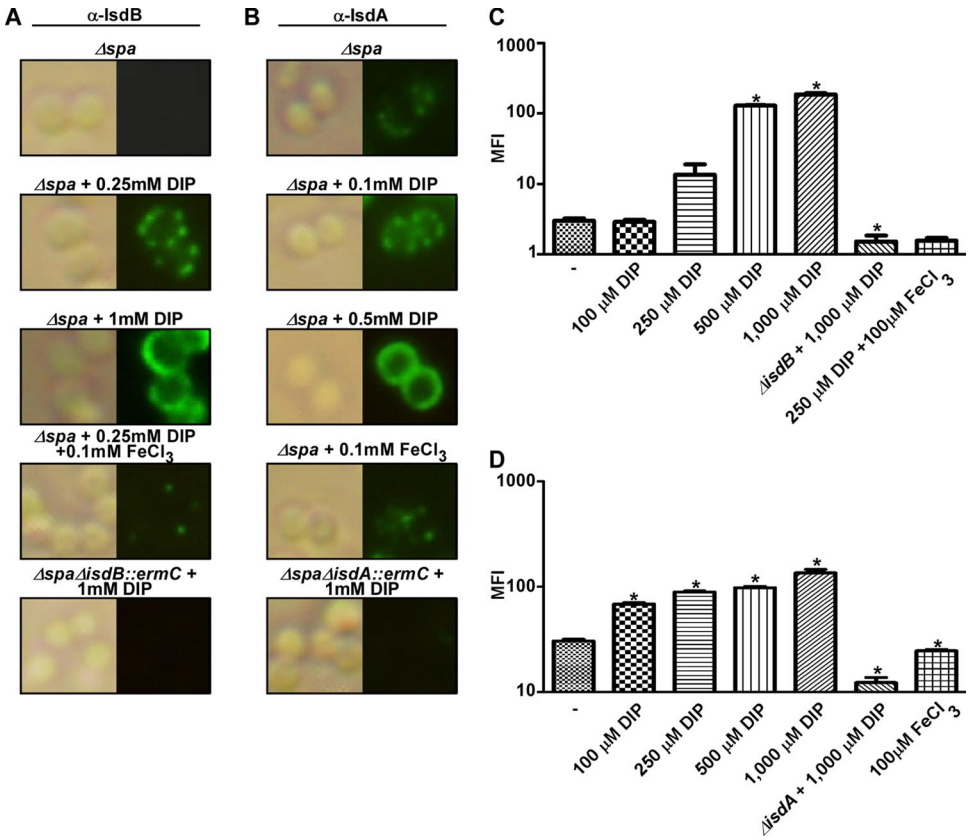

FIG. 2. Iron availability influences the expression and localization of IsdB and IsdA on the staphylococcal surface. Δ*spa* cells were grown overnight in medium supplemented with the indicated concentrations of DIP. (A and B) Bacteria were subsequently labeled with rabbit anti-IsdB (α-IsdB) (A) or rabbit anti-IsdA (B) antibodies, followed by Alexa Fluor 488 goat anti-rabbit IgG(H+L). (C and D) Quantification of relative amounts of IsdB (C) and IsdA (D) expressed on the surface of Δ*spa* cells was determined by FACS analysis. Asterisks indicate statistically significant differences in relation to Δ*spa* cells grown in plain TSB (−) as determined by a Student's *t* test ($P < 0.05$). In fluorescent images, green was increased by 100% in A and by 25% in B. MFI, mean fluorescence intensity.

using antisera specific for IsdA (Fig. 2B and D). We found that IsdA was expressed at low levels when grown under iron-sufficient conditions and that its level of expression increased upon iron starvation. Furthermore, we found that the distribution pattern of IsdA mirrored that of IsdB. When exposed to intermediate iron stress (100 μM DIP), IsdA localized to distinct puncta around the cells. In contrast, IsdA was evenly distributed around the cell wall in maximally iron-starved *S. aureus* cells (Fig. 2B). These results indicate that both the expression and subcellular distribution of IsdA and IsdB are regulated by iron availability and that the Isd system localizes to discrete regions within the cell under conditions of moderate iron stress.

Hemoglobin capture by *S. aureus* is iron regulated and IsdA/IsdB/IsdH dependent. The expression and surface distribution of IsdB is regulated by iron (Fig. 1), and IsdB has been shown to bind hemoglobin (13, 31, 46). In order to determine the effects that iron availability and IsdB expression have on hemoglobin binding to the surface of *S. aureus* cells, we analyzed hemoglobin binding to Δ*spa* cells grown under iron-replete or iron-depleted conditions. These experiments revealed that Δ*spa* cells grown under iron-replete conditions did not bind detectable levels of hemoglobin (Fig. 3A). However, when grown in the presence of the iron-chelating agent DIP, *S. aureus* cells exhibited a dose-dependent increase in levels of hemoglobin binding (Fig. 3B and C). Hemoglobin binding to the staphylococcal surface was localized to discrete puncta reminiscent of the iron-dependent distribution pattern observed for IsdB and IsdA (Fig. 2A and B). To assess whether the observed iron-dependent hemoglobin binding was mediated by IsdB, we measured hemoglobin binding to Δ*spa* Δ*isdB* cells (Fig. 3E to G). These experiments revealed that iron-starved Δ*spa* Δ*isdB* cells are deficient in binding hemoglobin compared to the Δ*spa* strain (Fig. 3G). To confirm that the punctate binding distribution of hemoglobin was not an artifact of antibody-based detection, we incubated bacteria with fluorescently labeled hemoglobin (see Fig. S1 in the supplemental material). This assay confirmed that hemoglobin binding to *S. aureus* is IsdB dependent and specific, as fluorescently labeled hemoglobin could be outcompeted by excess nonlabeled hemoglobin.

Despite the reduction in levels of hemoglobin binding, Δ*spa* Δ*isdB* cells were capable of binding detectable levels of hemoglobin in an iron-dependent manner (Fig. 3E and G). To confirm this observation, we measured relative hemoglobin binding to Δ*spa* and Δ*spa* Δ*isdB* cells grown under conditions of high or low iron with FACS (Fig. 3I). We observed that iron-starved Δ*spa* Δ*isdB* cells displayed a significant decrease in the

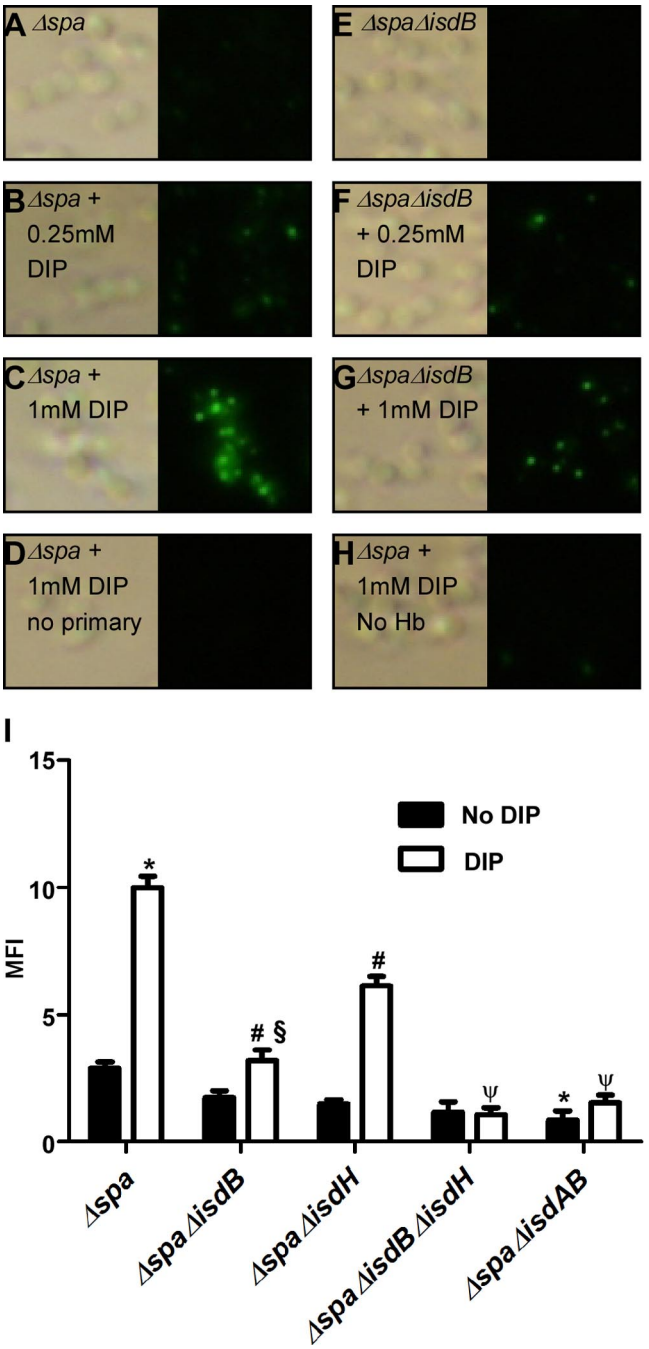

FIG. 3. Iron- and Isd-dependent hemoglobin binding to the surface of *S. aureus*. (A to G) Δ*spa* (A to D) or Δ*spa* Δ*isdB* (E to G) cells were grown overnight in TSB supplemented with the indicated concentrations of DIP. Bacteria were then incubated in PBS with human hemoglobin (Hb) and washed with PBS. Cells were subsequently labeled with mouse anti-hemoglobin IgG, followed by Alexa Fluor 488 goat anti-mouse IgG(H+L). (I) Quantification of the relative amounts of human hemoglobin bound to the surface of the indicated strains, grown in the presence of 1 mM DIP where indicated, determined by FACS. Error bars represent standard errors. The symbols indicate statistically significant differences as determined by a Student's *t* test ($P < 0.05$) in relation to the Δ*spa* strain with no DIP (*), the Δ*spa* strain with DIP (#), the Δ*spa* Δ*isdB* strain with no DIP (§), and the Δ*spa* Δ*isdB* strain with DIP (ψ).

level of hemoglobin binding compared to that of Δ*spa* cells. However, iron-starved Δ*spa* Δ*isdB* cells bound hemoglobin at levels higher than those of iron-replete Δ*spa* Δ*isdB* cells, suggesting the presence of an iron-regulated IsdB-independent hemoglobin binding activity (Fig. 3G and I). To date, IsdH and IsdA are the only staphylococcal proteins other than IsdB that have been shown to bind hemoglobin (7, 12, 36). To investigate whether IsdH was responsible for the residual levels of hemoglobin binding detected in Δ*spa* Δ*isdB* cells, we inactivated *isdH* in both the Δ*spa* and Δ*spa* Δ*isdB* backgrounds (creating the Δ*spa* Δ*isdH* and Δ*spa* Δ*isdB* Δ*isdH* strains, respectively) and measured the abilities of these strains to bind hemoglobin. When grown under iron-depleted conditions, Δ*spa* Δ*isdH* cells bound hemoglobin at reduced levels compared to those of Δ*spa* cells. Accordingly, Δ*spa* Δ*isdB* Δ*isdH* cells bound hemoglobin at lower levels than did Δ*spa* Δ*isdB* cells, suggesting that IsdH is at least partially responsible for the observed secondary binding activity. To assess whether IsdA contributes to capturing hemoglobin at the staphylococcal surface, we created a strain lacking *isdA* and *isdB* in the Δ*spa* background (Δ*spa* Δ*isdAB* strain) and tested the ability of the Δ*spa* Δ*isdAB* strain to bind hemoglobin. These experiments revealed that iron-starved Δ*spa* Δ*isdAB* cells exhibited decreased levels of hemoglobin binding compared to those of Δ*spa* and Δ*spa* Δ*isdB* cells. Furthermore, Δ*spa* Δ*isdAB* cells displayed decreased levels of hemoglobin binding compared to those of *S. aureus* cells grown under iron-replete conditions, suggesting that IsdA contributes to hemoglobin binding under both iron-replete and iron-depleted conditions (Fig. 3I). As a control for the specificity of the antihemoglobin antisera, we found that no strains stained positive for antibody binding in the absence of the hemoglobin addition (data not shown). These results indicate that IsdB is the primary hemoglobin receptor on the surface of *S. aureus* in iron-starved environments; however, IsdH and IsdA also contribute to hemoglobin capture.

We next sought to determine whether hemoglobin bound to the surface of staphylococci colocalizes with IsdB. To determine the relative localization of IsdB and hemoglobin, we grew Δ*spa* overnight under iron-depleted conditions and labeled the two molecules simultaneously on the surface of staphylococci with fluorophores emitting at distinct wavelengths. Both IsdB and hemoglobin displayed iron-dependent patterns of localization similar to that seen when labeled individually (Fig. 2A, 3C, and 4A). At 1 mM DIP, IsdB is diffusely distributed on the surface, whereas hemoglobin binding is punctate. Nevertheless, hemoglobin and IsdB colocalize on the surface, and hemoglobin binding is maximal in regions of the cell surfaces where IsdB is more abundant (Fig. 4A and B). Both IsdB and hemoglobin fluorescent labelings are specific, as indicated by the absence of the appropriate fluorescence when one of the primary antibodies is omitted (Fig. 4C and D). Cumulatively, these results suggest that hemoglobin binding to the surface of *S. aureus* is mediated by IsdB and occurs at distinct foci throughout the cell wall.

IsdA and IsdB form a complex at discrete regions within the cell wall. IsdB is capable of removing heme from hemoglobin and transferring it to IsdA in vitro (34, 50). In order for this process to occur in vivo, IsdA and IsdB, which are restrained to their anchoring site, are likely to be in direct proximity to each other. To test whether IsdA and IsdB colocalize on the surface

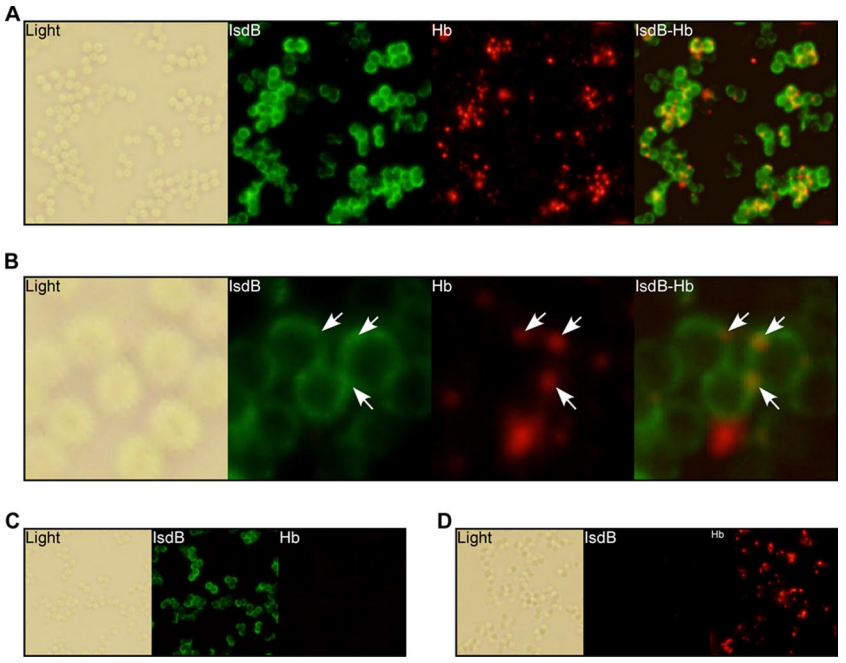

FIG. 4. Hemoglobin colocalizes with IsdB on the surface of *S. aureus*. (A) Δ*spa* cells were grown overnight in TSB supplemented with 1 mM DIP. Bacteria were then incubated with human hemoglobin (Hb) and washed with PBS. Cells were then simultaneously labeled with rabbit anti-IsdB and mouse anti-hemoglobin antibodies, followed by Alexa Fluor 488 goat anti-rabbit and Alexa Fluor 555 goat anti-mouse IgG(H+L). (B) Close-up of A. The arrows point to locations on the cell surface where hemoglobin is bound. To control for antibody cross-reactivity, either mouse anti-hemoglobin (C) or rabbit anti-IsdB (D) antibodies were omitted. In fluorescent images, green was increased by 25% and red was increased by 75%.

of *S. aureus* cells, we labeled the proteins simultaneously and viewed their localization using immunofluorescence. IsdB was detected using anti-IsdB counterstained with secondary 488 antibody, while IsdA was detected using biotinylated anti-IsdA counterstained with streptavidin-Alexa Fluor 555. These experiments revealed that IsdB labeling and IsdA labeling colocalize on the surface of *S. aureus* cells (Fig. 5A), suggesting that IsdA and IsdB are deposited proximally to each other within

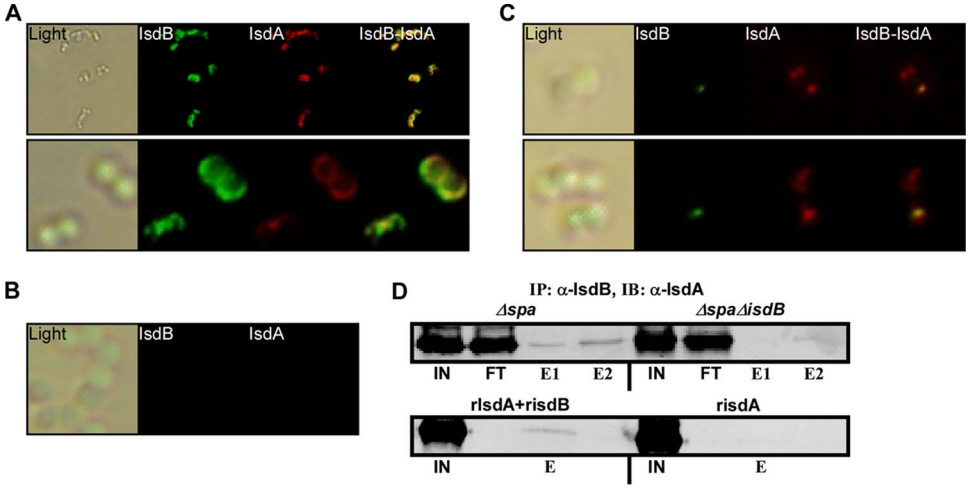

FIG. 5. IsdA and IsdB colocalize and interact on the cell wall of *S. aureus*. (A) Δ*spa* cells were grown overnight in TSB supplemented with 1 mM DIP. Bacteria were then sequentially labeled with rabbit anti-IsdB (α-IsdB), Alexa Fluor 488 goat anti-rabbit IgG(H+L), biotinylated rabbit anti-IsdA, and streptavidin Alexa Fluor 555 conjugate. (B and C) Cells from the same culture were subjected to trypsin digestion, washed, resuspended in TSB plus 1 mM DIP, and incubated. Aliquots were taken after 0 min (B) or 15 min (C) and labeled as described above (A). (D, top) Δ*spa* or Δ*spa* Δ*isdB* cells were grown overnight in TSB plus 1 mM DIP. The cell wall proteins were solubilized by lysostaphin. IsdB was pulled down with a Seize X protein A immunoprecipitation kit and rabbit anti-IsdB antibody. Input (IN), nonprecipitated flowthrough (FT), and eluted proteins (E1 and E2) were subjected to SDS-PAGE, transferred onto nitrocellulose, and immunoblotted (IB) with anti-IsdA antibody. (Bottom) rIsdA and rIsdB were combined and incubated at 37°C for 30 min. Immunoprecipitation (IP) was performed as described above (top), and input (IN) and elution (E) are shown.

the cell wall. To improve the resolution of this assay, we sought to determine the initial anchoring sites of IsdA and IsdB within the cell wall. To achieve this, we first treated staphylococci with trypsin, which effectively digested both IsdA and IsdB on the surface of staphylococci, as indicated by the absence of their labeling following treatment (Fig. 5B). The cells were then washed, resuspended in iron-deficient medium, and allowed to recover for 15 min. This assay enables the visualization of proteins that are newly deposited onto the cell wall, thus identifying the location of their anchoring. These experiments revealed that IsdA and IsdB are both deposited onto the same location on the surface of staphylococci (Fig. 5C). In addition, IsdA exhibits a slightly more-diffuse localization pattern, possibly due to its less-stringent regulation (Fig. 2). Among a total of 97 cells observed in this analysis, 81 cells (84%) deposited IsdA and IsdB at the same location. To confirm that IsdA and IsdB engage one another at these discrete anchoring sites, we performed immunoprecipitation of IsdB from cell wall lysates. Both IsdA and IsdB were precipitated by anti-IsdB, consistent with IsdAB complex formation occurring in the cell (Fig. 5D). Immunoprecipitation of lysates from Δ*spa* Δ*isdB* cells did not result in the precipitation of IsdA, confirming that IsdA pull-down requires IsdB. In further support of a physical interaction between IsdA and IsdB, rIsdA was immunoprecipitated with rIsdB by an anti-IsdB antibody following the incubation of these two proteins (Fig. 5D). These results indicate that IsdA and IsdB colocalize on the surface of staphylococci and that their colocalization is achieved through anchoring to the same site within the cell wall. Furthermore, these data suggest that IsdA and IsdB physically interact to promote hemoglobin capture during infection.

Newly formed IsdA and IsdB are anchored to the cell wall at the site of cell division. It has recently been shown that cell wall proteins in gram-positive bacteria are destined for two primary anchoring locations (3, 10). One destination is the site of cell division, where the new cell wall is rapidly synthesized, while the other is distant from the cell division site. In order to precisely determine the cell wall destinations of IsdA and IsdB, we utilized electron microscopy to localize immunogold-labeled IsdA and IsdB. Bacteria were grown in iron-depleted medium, treated with trypsin, and recovered in iron-depleted medium. Aliquots were taken before or immediately following trypsinization and at different time points after recovery. Bacteria were attached to nickel Formvar grids and labeled with anti-IsdB or anti-IsdA antibodies followed by anti-rabbit antibodies conjugated to 6-nm gold beads. Consistent with data acquired using immunofluorescence (Fig. 2A and B), both IsdA and IsdB were distributed throughout the cell surface when *S. aureus* cells were grown under maximally-iron-starved conditions (Fig. 6A and B and see Fig. S2 in the supplemental material). Gold beads were not detectable on the surface of Δ*spa* Δ*isdB* and Δ*spa* Δ*isdA* cells, indicating the specificity of the labeling procedure (Fig. 6C and see Fig. S2 in the supplemental material). Furthermore, gold beads were not detected following trypsin treatment of wild-type *S. aureus* cells grown under iron-deficient conditions, indicating that IsdA and IsdB are removed from the cell wall by trypsin digestion (Fig. 6D and see Fig. S2 in the supplemental material). Cells that were allowed to recover for 5 min following trypsinization displayed IsdB and IsdA deposition on the cell walls (Fig. 6E to L). Specifically, we observed localization of newly synthesized IsdA and IsdB to the site of cell division (Fig. 6I to K). In addition to localization at the site of new cell wall formation, IsdA was found more diffusely throughout the staphylococcal cell (Fig. 6I, J, and L). Bacteria that were allowed to recover for longer periods of time displayed progressively more-diffuse localization patterns of IsdA and IsdB, with uniform circumferential distribution following 60 min of recovery in iron-deficient medium (see Fig. S2 in the supplemental material). These data confirm that IsdA and IsdB are colocalized within the cell wall and establish the site of cell division as their common deposition location. However, it should be noted that the site of cell wall division does not appear to be the exclusive site of deposition for IsdA.

IsdA and IsdB exhibit organ-specific patterns of expression. Strains lacking IsdB exhibit decreased colonization of murine kidneys and spleen in systemic models of infection, and mice immunized with IsdB are protected against staphylococcal infection (27, 45, 46). These observations imply that IsdB is expressed within the vertebrate host. To test this directly, we monitored IsdB expression in a murine model of infection. C57BL/6J mice were infected with the Δ*spa* strain. After 96 h, the mice were sacrificed, and hearts were removed and homogenized with PBS. The homogenates were subjected to a series of centrifugations to remove larger mammalian cells and cellular debris. The resulting suspension was labeled with anti-IsdB antibody. Using this protocol, we recovered staphylococcal cells that bound anti-IsdB antibody, indicating an expression of IsdB on their surface. Heart tissue from an uninfected mouse processed in the same way did not stain positive for IsdB (Fig. 7A). These experiments demonstrate that IsdB is expressed during staphylococcal infection.

To quantify the relative expression levels of IsdB and IsdA during infection, we infected mice with wild-type *S. aureus*. After harvesting and processing the organs as described above, we normalized the samples to CFU of infecting *S. aureus* (see Materials and Methods). Following normalization, cell wall lysates were immunoblotted for the presence of IsdA and IsdB. As depicted in Fig. 7B, we detected IsdA both in livers and in hearts of infected mice but not in the organs of uninfected animals. In contrast, IsdB was detected in the hearts but not the livers of infected mice. Quantification of the band intensities from the samples of individual mice indicated lower levels of IsdA and IsdB expression in the livers of infected mice than in the hearts of the same animals (Fig. 7C). These experiments demonstrate that IsdB and IsdA are differentially expressed across organs.

To establish the contribution of IsdB to *S. aureus* virulence in hearts and livers, we infected mice with either the wild-type or Δ*isdB* strain. We observed a significant decrease in the virulence of the Δ*isdB* strain in the hearts, which was demonstrated by a reduction in CFU of invading bacteria by almost 2 orders of magnitude (Fig. 7D). Consistent with the lack of IsdB expression in murine livers, strains lacking IsdB colonized this organ as efficiently as the wild type (Fig. 7D). Together, these results demonstrate that *S. aureus* requires IsdB for growth in the murine heart and accordingly induces its expression when colonizing this organ. However, IsdB is not expressed during liver colonization and, hence, is dispensable for colonization in this host environment. This discrepancy in IsdA and IsdB expression and contribution to

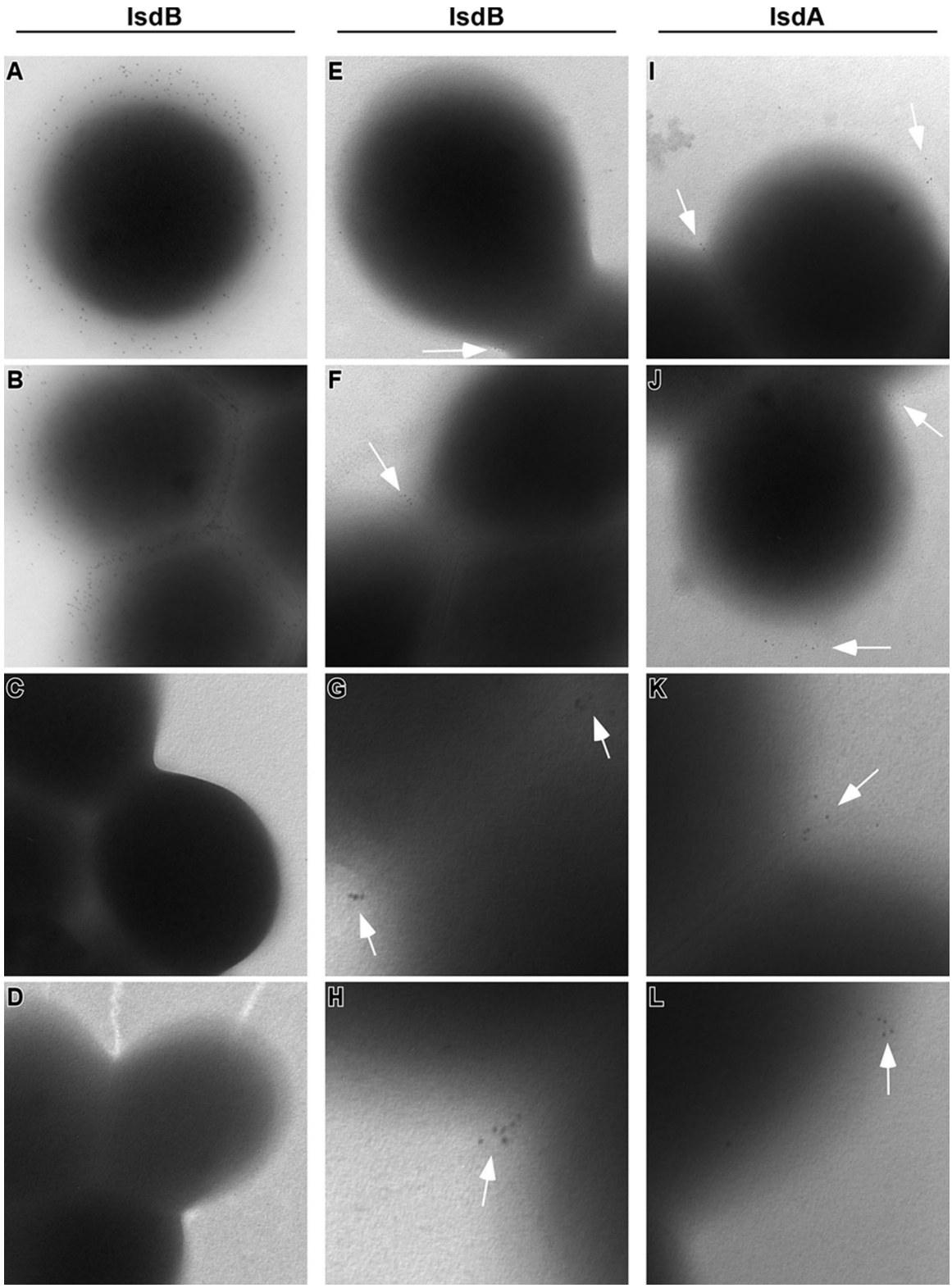

FIG. 6. IsdA and IsdB are anchored at sites of nascent cell wall formation. Δ*spa* cells were grown overnight in TSB supplemented with 1 mM DIP. Cells were treated with trypsin, washed, resuspended in TSB plus 1 mM DIP, and incubated. Aliquots were taken at different time points, washed, attached to nickel Formvar grids, and sequentially labeled with indicated primary antibodies and secondary 6-nm colloidal gold-Affinipure goat anti-rabbit IgG(H+L). (A and B) Nontrypsinized Δ*spa* cells labeled for IsdB. (C) Nontrypsinized Δ*spa* Δ*isdB* cells labeled for IsdB. (D) Trypsinized Δ*spa* cells labeled for IsdB. (E to L) Δ*spa* cells upon trypsin treatment and 5 min of recovery in TSB, labeled for IsdB (E to H) or IsdA (I to L).

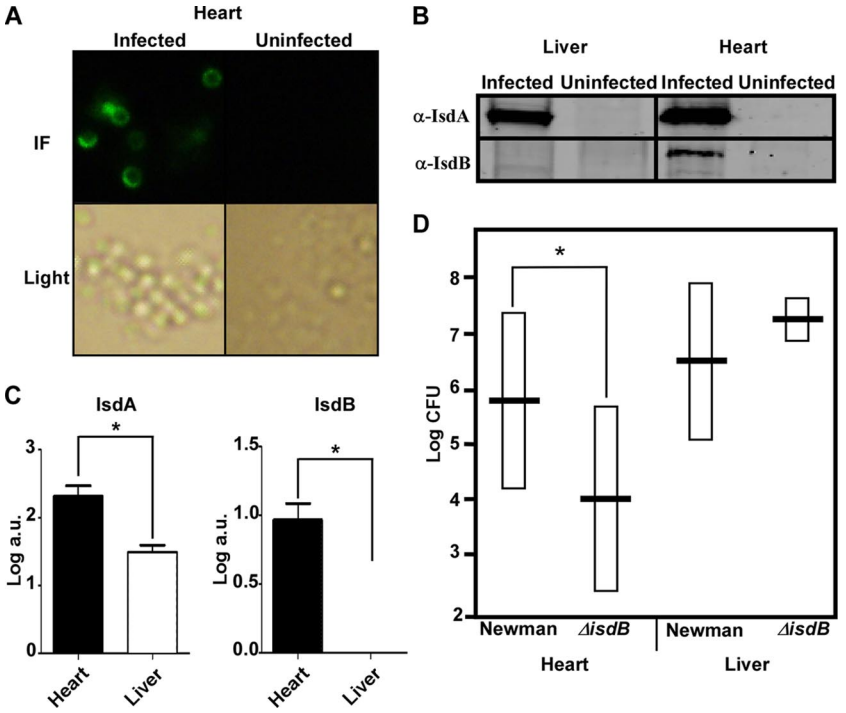

FIG. 7. IsdB is expressed within the hearts of infected animals and contributes to cardiac colonization. (A) C57BL/6J mice were retro-orbitally infected with 10^7 CFU of the Δ*spa* strain in 100 ml PBS and sacrificed 96 h postinfection. Hearts and livers were removed and homogenized in 1 ml sterile PBS. Bacteria were then partially separated from the mammalian cells by centrifugation, washed, and immunofluorescently labeled with anti-IsdB. IF, immunofluorescence. (B) Wild-type *S. aureus* cells recovered from the organs of C57BL/6J mice were separated from the mammalian cells as described above (A), normalized to 1×10^5 CFU, lysed with lysostaphin to release cell wall proteins that were separated on SDS-PAGE gels, and transferred onto a nitrocellulose membrane. The membrane was immunoblotted with anti-IsdA (α-IsdA) and anti-IsdB antibodies. (C) Relative amounts of IsdA and IsdB in the infected organs were quantified based on immunoblot intensity. Error bars represent standard errors. Asterisks indicate statistically significant differences as determined by a Student's *t* test ($P < 0.05$). a.u., arbitrary units. (D) Organ colonization was estimated based on CFU quantification by serial dilution and plating onto tryptic soy agar. The horizontal bars represent the means, and boxes represent standard deviations. Asterisks indicate statistically significant differences as determined by a Student's *t* test ($P < 0.05$). Each group included at least nine mice.

infection is potentially due to differences in iron availability within the hearts and livers of mice.

DISCUSSION

In this report, we demonstrate the subcellular colocalization and interaction of IsdA and IsdB, which function together to provide nutrient heme iron to *S. aureus* during infection. Due to the requirement for iron in numerous physiological processes, its acquisition is an important task for all living organisms. Mammals have adapted to exploit the necessity of iron for microbial replication by sequestering it away from microbes that have breached the skin or mucosal layers. This is achieved primarily by concealing elemental iron from microbial invaders within host cells and iron-sequestering proteins (11). Pathogens in turn have evolved mechanisms to remove iron from host proteins and internalize it for their own uses (9). In gram-positive bacteria, the thick cell wall poses an additional obstacle to the transport of iron (38, 44). To acquire iron during infection, *S. aureus* utilizes the Isd system, which allows it to bind hemoglobin and remove and transport heme across the cell wall and membrane into the cytoplasm, where heme is degraded to release iron (44). The properties of individual factors constituting the Isd system have been investigated; however, the mechanics of their cooperation remain to be established. Recent studies have shown that rIsdB is capable of removing heme from hemoglobin and passing it to rIsdA in solution (34, 50). In vivo, IsdA and IsdB are predicted to be located in direct proximity to each other in order to remove and pass heme iron. Testing this model has proven difficult due to the inherent complexities associated with performing protein localization studies with *S. aureus*. Few reports on the localization of *S. aureus* proteins have been published to date due to the small size of staphylococcal cells and the nonspecific binding of IgG by protein A.

Here we demonstrate that IsdA and IsdB expression and localization are regulated by iron availability. Under conditions in which their expression is limited, IsdA and IsdB are concentrated to distinct puncta located throughout the cell surface. One possible explanation for this organized localization pattern is that under these conditions, the Isd proteins are produced in successive waves of expression and are therefore anchored to the cell wall periodically. Another mechanism through which punctate localization could be achieved is suggested by the location of IsdA and IsdB deposition at the sites of cell division, possibly through a single secretion portal. Because cell division is periodic, it is possible that when the cell starts dividing, this portal "opens," and all synthesized IsdB swiftly gets incorporated into the cell wall. A "pause" follows, during which the IsdB levels are exhausted, and it is not incor-

porated into the cell wall, accounting for the interruptions in its distribution. Although these models are speculative at this point, the proteins of the Isd system provide excellent tools to test these models, because their expression levels are easily manipulated by iron availability.

In this study, we have shown that IsdA and IsdB are deposited at the same location on the cell wall of *S. aureus*. This might ensure that IsdA and IsdB, which function together in heme import, are proximal to each other. Notably, some IsdA is deposited on the cell wall at locations distant from IsdB, which might be due to the fact that IsdA has functions distinct from heme iron acquisition, such as resistance to antimicrobials and adherence to the host epithelium (5–7). Recent studies indicated that not all cell wall proteins of gram-positive bacteria are destined for the same site, suggesting differential localizations of surface proteins depending on their functions (3, 10, 41). In keeping with this finding, the specific deposition of IsdB at the cell division site can be attributed to the YSIRK/GS sequence found within its signal peptide domain, which primes cell wall-anchored proteins to sites of cell division (3, 10). In contrast, IsdA does not encode YSIRK/GS within its signal peptide and is anchored to sites both within and outside the sites of cell division. These facts suggest that additional factors which contribute to the localization of cell wall anchoring are yet to be determined. It is possible that IsdA anchoring is not restricted to the site of cell division due to its higher basal level of expression. In addition to spatial proximity, the possibility that IsdA and IsdB interact in vivo is supported by the observation that IsdA coimmunoprecipitates with IsdB.

A primary function of the Isd system is to capture hemoglobin for use as a nutrient iron source. We have found that hemoglobin binding to the surface of *S. aureus* depends on iron availability and the presence of IsdB. Surprisingly, staphylococci, which are maximally iron starved and therefore display IsdB uniformly throughout the cell surface, bind hemoglobin at discrete locales. It is possible that in order to effectively bind hemoglobin, multiple tightly packed molecules of IsdB are employed, or it is possible that IsdB requires another factor to bind hemoglobin, and this factor is present only at these locales. Additionally, we observed an iron-dependent, IsdB-independent hemoglobin binding activity conferred by IsdA and IsdH, consistent with their in vitro hemoglobin binding activity (7, 12, 36). Interestingly, the Δ*spa* Δ*isdAB* strain was impaired in its ability to bind hemoglobin when grown in iron-rich medium compared to the Δ*spa* strain. This indicates that IsdA binds minimal levels of hemoglobin under iron-sufficient conditions, potentially providing *S. aureus* with a mechanism to acquire low levels of heme when the organism is not in an iron-starved state.

Levels of IsdA and IsdB expressed by *S. aureus* cells isolated from the hearts of infected mice are lower than those of "maximally starved" bacteria grown in TSB plus 1 mM DIP (data not shown). By comparing the expression pattern of IsdB from *S. aureus* grown in iron-deplete medium to that of IsdB from *S. aureus* removed from infected animals, we can estimate that *S. aureus* cells experience a level of iron starvation within the heart similar to that seen upon growth in TSB plus 250 μM DIP. Furthermore, IsdB is not uniformly localized on the surface of bacterial cells removed directly from infected organs. These results suggest that the punctate localization of IsdB observed in our in vitro experiments is recapitulated during staphylococcal infection.

Consistent with the observation that IsdB is expressed by *S. aureus* in the hearts but not the livers of infected mice, the Δ*isdB* strain is impaired in colonizing the heart, while this strain colonizes livers at levels equivalent to those of the wild type. The level of expression of IsdA is also lower in murine livers than in hearts. Taking into consideration the various degrees by which iron impacts the regulation of IsdB and IsdA, we suggest that the heart provides an environment with less available iron than that found in the liver. This idea is supported by the fact that the liver is the major storage site for iron in vertebrates (17, 18). Furthermore, the liver is a common site of *S. aureus*-induced abscess formation, and iron overload is associated with increased susceptibility to staphylococcal liver infection (4, 42). It has recently been shown that *S. aureus* cells recovered from murine airways bind considerable amounts of hemoglobin, suggesting that the respiratory tract is an iron-poor environment similar to the heart (48). In addition, we have found that *S. aureus* is iron deficient when inside murine kidney abscesses (37). Thus, monitoring of the levels of expression of Isd proteins and hemoglobin binding across murine organs can be used to predict the level of iron restriction experienced by *S. aureus* during the course of an infection. Heme iron acquisition systems have been considered to be viable targets for novel antimicrobials and antistaphylococcal vaccines (27, 45). The differential expression of these systems across organs should be taken into consideration when designing future therapeutic and preventive regimens.

ACKNOWLEDGMENTS

This work was supported by U.S. Public Health Service grant AI69233 from the National Institute of Allergy and Infection Diseases (E.P.S.). E.P.S. is a Searle Scholar and holds an Investigator in Pathogenesis of Infectious Disease award from the Burroughs Wellcome Fund. Experiments were performed in part through the use of the VUMC Research EM Resource (sponsored by NIH grants DK20539, CA68485, and DK58404).

We thank Jay Jerome and Denny Kerns for assistance and advice in performing electron microscopy. We also thank the members of the Skaar laboratory for critical reading of the manuscript.

REFERENCES

1. **Bae, T., and O. Schneewind.** 2006. Allelic replacement in *Staphylococcus aureus* with inducible counter-selection. Plasmid **55:**58–63.
2. **Bullen, J. J., and E. Griffiths.** 1999. Iron and infection: molecular, physiological and clinical aspects. John Wiley & Sons, New York, NY.
3. **Carlsson, F., M. Stalhammar-Carlemalm, K. Flardh, C. Sandin, E. Carlemalm, and G. Lindahl.** 2006. Signal sequence directs localized secretion of bacterial surface proteins. Nature **442:**943–946.
4. **Christou, L., G. Pappas, and M. E. Falagas.** 2007. Bacterial infection-related morbidity and mortality in cirrhosis. Am. J. Gastroenterol. **102:**1510–1517.
5. **Clarke, S. R., and S. J. Foster.** 2008. IsdA protects *Staphylococcus aureus* against the bactericidal protease activity of apolactoferrin. Infect. Immun. **76:**1518–1526.
6. **Clarke, S. R., R. Mohamed, L. Bian, A. F. Routh, J. F. Kokai-Kun, J. J. Mond, A. Tarkowski, and S. J. Foster.** 2007. The *Staphylococcus aureus* surface protein IsdA mediates resistance to innate defenses of human skin. Cell Host Microbe **1:**199–212.
7. **Clarke, S. R., M. D. Wiltshire, and S. J. Foster.** 2004. IsdA of *Staphylococcus aureus* is a broad spectrum, iron-regulated adhesin. Mol. Microbiol. **51:**1509–1519.
8. **Crichton, R.** 2001. Inorganic biochemistry of iron metabolism: from molecular mechanisms to clinical consequences, vol. 2. John Wiley & Sons, Ltd., West Sussex, England.
9. **Crosa, J. H., A. R. May, and S. M. Payne.** 2004. Iron transport in bacteria. ASM Press, Washington, DC.
10. **DeDent, A., T. Bae, D. M. Missiakas, and O. Schneewind.** 2008. Signal

peptides direct surface proteins to two distinct envelope locations of *Staphylococcus aureus*. EMBO J. **27:**2656–2668.
11. **Drabkin, D.** 1951. Metabolism of the hemin chromoproteins. Physiol. Rev. **31:**345–431.
12. **Dryla, A., D. Gelbmann, A. Von Gabain, and E. Nagy.** 2003. Identification of a novel iron regulated staphylococcal surface protein with haptoglobin-haemoglobin binding activity. Mol. Microbiol. **49:**37–53.
13. **Dryla, A., B. Hoffmann, D. Gelbmann, C. Giefing, M. Hanner, A. Meinke, A. S. Anderson, W. Koppensteiner, R. Konrat, A. von Gabain, and E. Nagy.** 2007. High-affinity binding of the staphylococcal HarA protein to haptoglobin and hemoglobin involves a domain with an antiparallel eight-stranded β-barrel fold. J. Bacteriol. **189:**254–264.
14. **Flock, J. I., G. Froman, K. Jonsson, B. Guss, C. Signas, B. Nilsson, G. Raucci, M. Hook, T. Wadstrom, and M. Lindberg.** 1987. Cloning and expression of the gene for a fibronectin-binding protein from *Staphylococcus aureus*. EMBO J. **6:**2351–2357.
15. **Forsgren, A., and U. Forsum.** 1970. Role of protein A in nonspecific immunofluorescence of *Staphylococcus aureus*. Infect. Immun. **2:**387–391.
16. **Forsgren, A., and J. Sjoquist.** 1966. "Protein A" from *S. aureus*. I. Pseudoimmune reaction with human gamma-globulin. J. Immunol. **97:**822–827.
17. **Ganz, T.** 2007. Molecular control of iron transport. J. Am. Soc. Nephrol. **18:**394–400.
18. **Graham, R. M., A. C. Chua, C. E. Herbison, J. K. Olynyk, and D. Trinder.** 2007. Liver iron transport. World J. Gastroenterol. **13:**4725–4736.
19. **Grigg, J. C., C. L. Vermeiren, D. E. Heinrichs, and M. E. Murphy.** 2007. Haem recognition by a *Staphylococcus aureus* NEAT domain. Mol. Microbiol. **63:**139–149.
20. **Grigg, J. C., C. L. Vermeiren, D. E. Heinrichs, and M. E. Murphy.** 2007. Heme coordination by *Staphylococcus aureus* IsdE. J. Biol. Chem. **282:**28815–28822.
21. **Jonsson, I. M., S. K. Mazmanian, O. Schneewind, T. Bremell, and A. Tarkowski.** 2003. The role of *Staphylococcus aureus* sortase A and sortase B in murine arthritis. Microbes Infect. **5:**775–780.
22. **Jonsson, I. M., S. K. Mazmanian, O. Schneewind, M. Verdrengh, T. Bremell, and A. Tarkowski.** 2002. On the role of *Staphylococcus aureus* sortase and sortase-catalyzed surface protein anchoring in murine septic arthritis. J. Infect. Dis. **185:**1417–1424.
23. **Klein, E., D. L. Smith, and R. Laxminarayan.** 2007. Hospitalizations and deaths caused by methicillin-resistant *Staphylococcus aureus*, United States, 1999–2005. Emerg. Infect. Dis. **13:**1840–1846.
24. **Klevens, R. M., M. A. Morrison, J. Nadle, S. Petit, K. Gershman, S. Ray, L. H. Harrison, R. Lynfield, G. Dumyati, J. M. Townes, A. S. Craig, E. R. Zell, G. E. Fosheim, L. K. McDougal, R. B. Carey, and S. K. Fridkin.** 2007. Invasive methicillin-resistant *Staphylococcus aureus* infections in the United States. JAMA **298:**1763–1771.
25. **Kuehnert, M. J., H. A. Hill, B. A. Kupronis, J. I. Tokars, S. L. Solomon, and D. B. Jernigan.** 2005. Methicillin-resistant-*Staphylococcus aureus* hospitalizations, United States. Emerg. Infect. Dis. **11:**868–872.
26. **Kuehnert, M. J., D. Kruszon-Moran, H. A. Hill, G. McQuillan, S. K. McAllister, G. Fosheim, L. K. McDougal, J. Chaitram, B. Jensen, S. K. Fridkin, G. Killgore, and F. C. Tenover.** 2006. Prevalence of *Staphylococcus aureus* nasal colonization in the United States, 2001–2002. J. Infect. Dis. **193:**172–179.
27. **Kuklin, N. A., D. J. Clark, S. Secore, J. Cook, L. D. Cope, T. McNeely, L. Noble, M. J. Brown, J. K. Zorman, X. M. Wang, G. Pancari, H. Fan, K. Isett, B. Burgess, J. Bryan, M. Brownlow, H. George, M. Meinz, M. E. Liddell, R. Kelly, L. Schultz, D. Montgomery, J. Onishi, M. Losada, M. Martin, T. Ebert, C. Y. Tan, T. L. Schofield, E. Nagy, A. Meineke, J. G. Joyce, M. B. Kurtz, M. J. Caulfield, K. U. Jansen, W. McClements, and A. S. Anderson.** 2006. A novel *Staphylococcus aureus* vaccine: iron surface determinant B induces rapid antibody responses in rhesus macaques and specific increased survival in a murine *S. aureus* sepsis model. Infect. Immun. **74:**2215–2223.
28. **Lee, W. C., M. L. Reniere, E. P. Skaar, and M. E. Murphy.** 2008. Ruffling of metalloporphyrins bound to IsdG and IsdI, two heme-degrading enzymes in *Staphylococcus aureus*. J. Biol. Chem. **283:**30957–30963.
29. **Lowy, F. D.** 2007. Secrets of a superbug. Nat. Med. **13:**1418–1420.
30. **Mazmanian, S. K., G. Liu, E. R. Jensen, E. Lenoy, and O. Schneewind.** 2000. *Staphylococcus aureus* sortase mutants defective in the display of surface proteins and in the pathogenesis of animal infections. Proc. Natl. Acad. Sci. USA **97:**5510–5515.
31. **Mazmanian, S. K., E. P. Skaar, A. H. Gaspar, M. Humayun, P. Gornicki, J. Jelenska, A. Joachmiak, D. M. Missiakas, and O. Schneewind.** 2003. Passage of heme-iron across the envelope of *Staphylococcus aureus*. Science **299:**906–909.
32. **Mazmanian, S. K., H. Ton-That, K. Su, and O. Schneewind.** 2002. An iron-regulated sortase anchors a class of surface protein during *Staphylococcus aureus* pathogenesis. Proc. Natl. Acad. Sci. USA **99:**2293–2298.
33. **McDevitt, D., P. Francois, P. Vaudaux, and T. J. Foster.** 1994. Molecular characterization of the clumping factor (fibrinogen receptor) of *Staphylococcus aureus*. Mol. Microbiol. **11:**237–248.
34. **Muryoi, N., M. T. Tiedemann, M. Pluym, J. Cheung, D. E. Heinrichs, and M. J. Stillman.** 2008. Demonstration of the iron-regulated surface determinant (Isd) heme transfer pathway in *Staphylococcus aureus*. J. Biol. Chem. **283:**28125–28136.
35. **O'Brien, L., S. W. Kerrigan, G. Kaw, M. Hogan, J. Penades, D. Litt, D. J. Fitzgerald, T. J. Foster, and D. Cox.** 2002. Multiple mechanisms for the activation of human platelet aggregation by *Staphylococcus aureus*: roles for the clumping factors ClfA and ClfB, the serine-aspartate repeat protein SdrE and protein A. Mol. Microbiol. **44:**1033–1044.
36. **Pilpa, R. M., S. A. Robson, V. A. Villareal, M. L. Wong, M. Phillips, and R. T. Clubb.** 2008. Functionally distinct NEAT (NEAr transporter) domains within the *Staphylococcus aureus* IsdH/HarA protein extract heme from methemoglobin. J. Biol. Chem. **284:**1166–1176.
37. **Reniere, M. L., and E. P. Skaar.** 2008. *Staphylococcus aureus* haem oxygenases are differentially regulated by iron and haem. Mol. Microbiol. **69:**1304–1315.
38. **Reniere, M. L., V. J. Torres, and E. P. Skaar.** 2007. Intracellular metalloporphyrin metabolism in *Staphylococcus aureus*. Biometals **20:**333–345.
39. **Roche, F. M., R. Massey, S. J. Peacock, N. P. Day, L. Visai, P. Speziale, A. Lam, M. Pallen, and T. J. Foster.** 2003. Characterization of novel LPXTG-containing proteins of *Staphylococcus aureus* identified from genome sequences. Microbiology **149:**643–654.
40. **Roche, F. M., M. Meehan, and T. J. Foster.** 2003. The *Staphylococcus aureus* surface protein SasG and its homologues promote bacterial adherence to human desquamated nasal epithelial cells. Microbiology **149:**2759–2767.
41. **Rosch, J. W., and M. G. Caparon.** 2005. The ExPortal: an organelle dedicated to the biogenesis of secreted proteins in *Streptococcus pyogenes*. Mol. Microbiol. **58:**959–968.
42. **Singh, N., C. Wannstedt, L. Keyes, D. Mayher, L. Tickerhoof, M. Akoad, M. M. Wagener, R. Frye, and T. V. Cacciarelli.** 2007. Hepatic iron content and the risk of *Staphylococcus aureus* bacteremia in liver transplant recipients. Prog. Transplant. **17:**332–336.
43. **Skaar, E. P., A. H. Gaspar, and O. Schneewind.** 2004. IsdG and IsdI, heme-degrading enzymes in the cytoplasm of *Staphylococcus aureus*. J. Biol. Chem. **279:**436–443.
44. **Skaar, E. P., and O. Schneewind.** 2004. Iron-regulated surface determinants (Isd) of *Staphylococcus aureus*: stealing iron from heme. Microbes Infect. **6:**390–397.
45. **Stranger-Jones, Y. K., T. Bae, and O. Schneewind.** 2006. Vaccine assembly from surface proteins of *Staphylococcus aureus*. Proc. Natl. Acad. Sci. USA **103:**16942–16947.
46. **Torres, V. J., G. Pishchany, M. Humayun, O. Schneewind, and E. P. Skaar.** 2006. *Staphylococcus aureus* IsdB is a hemoglobin receptor required for heme iron utilization. J. Bacteriol. **188:**8421–8429.
47. **Umbreit, J.** 2007. Methemoglobin—it's not just blue: a concise review. Am. J. Hematol. **82:**134–144.
48. **Ventura, C. L., R. Higdon, E. Kolker, S. J. Skerrett, and C. E. Rubens.** 2008. Host airway proteins interact with *Staphylococcus aureus* during early pneumonia. Infect. Immun. **76:**888–898.
49. **Weiss, W. J., E. Lenoy, T. Murphy, L. Tardio, P. Burgio, S. J. Projan, O. Schneewind, and L. Alksne.** 2004. Effect of *srtA* and *srtB* gene expression on the virulence of *Staphylococcus aureus* in animal models of infection. J. Antimicrob. Chemother. **53:**480–486.
50. **Zhu, H., G. Xie, M. Liu, J. S. Olson, M. Fabian, D. M. Dooley, and B. Lei.** 2008. Pathway for heme uptake from human methemoglobin by the iron-regulated surface determinants system of *Staphylococcus aureus*. J. Biol. Chem. **283:**18450–18460.

Editor: A. Camilli